doi.org/10.36721/PJPS.2025.38.2.REG.12516.1

Effect of azithromycin-conjugated gold and silver nanoparticles on the cytotoxicity of hepatocellular cancer cells

Dabeeran Zehra[1], Shumaila Usman[2]*, Almas Jabeen[3], Kauser Ismail[4], Zahida Memon[4], Zara Aslam[5] and Muhammad Raza Shah[5]

[1]Department of Pharmacology, Dow University of Health Sciences (DUHS), Baba-e-Urdu Road, Karachi, Pakistan
[2]Department of Research, Ziauddin University, 4/B, Shahrah-e-Ghalib, Block 6, Clifton Karachi
[3]Dr. Panjwani Centre for Molecular Medicine and Drug research, International Centre for Chemical and Biological Sciences, University of Karachi
[4]Department of Pharmacology, Ziauddin University, 4/B, Shahrah-e-Ghalib, Block 6, Clifton Karachi
[5]H.E.J. Research Institute of Chemistry, International Centre for Chemical and Biological Sciences, University of Karachi

Abstract: Azithromycin is a member of macrolide antibiotics, and has been reported to inhibit the proliferation of cancer cells. Nanoparticles particularly nanometals have been recently investigated in cancer chemotherapy owing to their enhanced pharmacokinetic and pharmacodynamic profile over conventional preparations due to nanoscale size and unique physicochemical characteristics. Therefore, this study is intended to explore the role of silver and gold metallic form of an antibiotic Azithromycin (AZM) in exhibiting the anticancer activity against hepatocellular carcinoma cell line (HepG2). After synthesis, Azithromycin conjugated gold and silver nanoparticles were characterized by UV-visible spectroscopy, Fourier transform infrared analysis, Atomic force microscopy and Zeta sizer and zeta potential analysis. HepG2 cells treated with Azithromycin, Gold conjugated Azithromycin (Au-AZM) and Silver conjugated Azithromycin (Ag-AZM) were analyzed for cytotoxic activity via MTT assay and apoptotic potential via nuclear area factor calculation made after processing DAPI stained images. The cytotoxicity data showed that Silver conjugated Azithromycin showed more inhibitory effect (IC_{50}= 33.3µg/ml) on proliferation of HepG2 cells as compare to Gold conjugated Azithromycin (IC_{50}= 78.3µg/ml) and Azithromycin alone (IC_{50}=88.8µg/ml) respectively. Similarly, the Silver conjugated Azithromycin group showed enhanced apoptosis in comparison with Gold conjugated Azithromycin and Azithromycin. In conclusion, this study proposes a potent role of Silver conjugated Azithromycin in attenuation of hepatocellular cancer cell growth, nevertheless further *in vivo* and clinical trials are required in order to mark its significance as a therapeutic agent.

Keywords: Anticancer effects, Azithromycin, cytotoxic analysis, gold and silver nano conjugation, hepatocellular carcinoma

INTRODUCTION

Due to serious obstacles towards development of novel cancer chemotherapeutic options, the strategies based on active targeting such as nanomedicine are being employed in number of studies (Alrushaid *et al*, 2023). Owing to specific physicochemical properties in terms of size and surface charge, nanocarriers are expected to revolutionize the cancer treatment by contributing in modifications of pharmacokinetics and pharmacodynamics of conventional chemotherapeutics which could be highly beneficial in reducing the toxicity of later (Chatterjee and Kumar, 2022). The extensivity carried by the nanoparticles is largely due to their small particle size because of which they are able to accumulate preferentially in tumor sites as the tumor blood vessel is leakier and more fenestrated. The enhanced permeability of vasculature coupled with the impaired lymphatic drainage in rapidly growing tumors directed the concept of enhanced permeability and retention effect (EPR) of the nanoparticle size (Tian *et al*, 2022). Literature suggests their role in facilitation of drug administration in bit lower doses as the conjugated drugs remain protected from detrimental environmental factors such as body pH, enzyme digestion and possible biochemical modifications (Abbaszadeh *et al*., 2019). One of the most useful nano-formulations are nanometals, being available as platinum, gold, silver or iron-based nanoparticles which have been tested successfully on different *in-vitro* and *in-vivo* models with promising anticancer findings (Khursheed *et al*., 2022). A monumental research published in this regard was conducted as a phase I clinical trials with gold nanoparticle bound to the recombinant-human TNFα which render previously toxic doses to nontoxic (Liu *et al*, 2022). Like AuNPs, silver nanoparticles (AgNPs) are also being considered influential with regard to their anticancer properties where most of the studies have mentioned the apoptotic potential of silver particles (Baranwal *et al*, 2023). Nanometals are under continuous investigation for cancer chemotherapy being conjugated with conventional and novel drugs as well as repurposed drugs such as antibiotics. Macrolides are one such group of semi synthetic antibiotics, that has demonstrated to produce diverse effects, like anti-inflammatory, immunomodulatory (Xu *et al*, 2022), anti-oxidative and

Corresponding author: e-mail: dabeeran519@gmail.com

anticancer effects on eukaryotes beside their property to inhibit protein synthesis in prokaryote (Shariatzadeh *et al*, 2022). Another critical and favorable feature of these antibiotics is that, most of them are non-toxic for normal cells thus most likely to exert minimal adverse effects when compared to anticancer agents. Therefore, good number of researches have been macrolides such as Clarithromycin (CAM) and Azithromycin (AZM) on different cancer cell lines to repurpose macrolides for cancer treatment both as alternative or as adjuvant, alone or in combination via detailed inquisition of their molecular mechanisms (Qiao *et al*., 2018).

Hepatocellular carcinoma is one of the commonly occuring cancer in Pakistan associated with high metastatic potential and limited treatment options (Tahir *et al*, 2022). Unfortunately, majority of the patients present with advanced stages where the only option is treatment with oral chemotherapeutic agent i.e, Sorafenib which is not as much effective secondary to its limited overall survival time and serious adverse effects (Pang *et al*, 2022).

In line with these facts, this study is designed to appraise the cytotoxic activities of gold and silver nanometallic forms of Azithromycin on HepG2 cells.

MATERIALS AND METHODS

This was an *in-vitro* experimental study which was conducted after institutional approval from Ethical Review Committee, Ziauddin University (Reference code: 0750119DZPHA).

Materials and instruments

Tetrachloroauric (III) acid trihydrate (99%), Silver nitrate (99%), azithromycin (95%) and sodium borohydride (97%) were acquired from Sigma-Aldrich Inc, USA. All solutions were made through Deionized water. UV-Visible spectroscopic analysis was performed by Shimadzu double beam UV-1800 spectrophotometer bearing a path length of 1 cm. A Bruker Vector 22 FT-IR spectrometer was utilized to attain the Fourier Transform Infrared (FT-IR) spectrum at room temperature, within the range of 4000-400 cm^{-1}. For morphological analysis of nano-particles, Atomic Force Microscope (Agilent 5500) operated in tapping mode has been used. Zetasizer *Nano ZSP (*Malvern) was employed for determination of the average particles size and zeta potential of the tested compounds. VWR symphony ultrasonicator-2316 was used for sonication.

Synthesis of azithromycin coated gold and silver nanoparticles

Synthesis of AZM conjugated gold and silver nano-particles was done at *Third World Center for Chemical Sciences* (TWC), *International Center for Chemical and Biological Sciences (ICCBS), University of Karachi, Pakistan* by $NaBH_4$ reduction method reported in the literature (Male *et al*., 2008) (Zhang *et al*., 2018). Briefly, AZM stock solution (2mg/mL) was constituted in methanol-water (1:1) while aqueous tetrachloroauric (III) acid trihydrate ($HAuCl_4$) and silver nitrate ($AgNO_3$) was costituted at a concentration of 0.1mM. AZM solution of 2mL (2mg/mL) was added dropwise in 2mL (0.1mM) of tetrachloroauric (III) acid trihydrate and silver nitrate solution separately under constant stirring (200 rpm) at room temperature. After 10 minutes, 10µL of freshly prepared aqueous $NaBH_4$ (5mM) solution was added in to both reaction mixture which was followed by rapid colour change from translucent to ruby red for gold particles while for silver particles it turned to yellow. The samples were subjected for UV-Visible spectroscopy for the evaluation of surface plasmon resonance (SPR) band of AZM conjugated nanoparticles along with Fourier transform infrared analysis (FTIR), Atomic force microscopy (AFM) and zeta sizer and potential analysis for definite characterization.

Drug/compound preparation

Sterile 100% DMSO has been used for the preparation of stock concentrations of AZM (Thermo Scientific USA) while for silver and gold conjugated forms of AZM, ethanol was used. Then different working solutions from these drug groups were newly constituted from stock solutions after making the dilutions of stock in Dulbecco modified Eagle medium (DMEM) (Thermo Scientific USA). HepG2 cells were treated with various working concentrations of both AZM alone and its conjugated forms after optimization.

Cell cultures

HepG2 cell line of ATCC, Manassas USA, was generously provided by Biobank facility of *Dr. Panjwani center for molecular medicine and drug research (PCMD), International Center for Chemical and Biological Sciences (ICCBS), University of Karachi, Pakistan*,. All the chemicals were purchased from Thermo Scientific, USA. 75 cc flask were used for culturing the cells. DMEM added with 1% L-glutamine (and 10% FBS), 1% penicillin and streptomycin, in humidified atmosphere keeping the temperature at 37°C comprising 5% CO_2. Once the cells attained confluency to 80%, they were detached via 0.05% trypsin followed by cell counting through trypan blue on hemocytometer slide under Floid cell imaging system, Thermo scientific, USA.

MTT cytotoxic assay

We employed MTT colorimetric assay which is a standard method for determining the cytotoxicity of AZM, Au-AZM and Ag-AZM. Firstly 30,000 cells/well growing exponentially immersed in complete DMEM were seeded in 96-wells flat bottom cell culture-treated plate. Cells were incubated for subsequent 24 hrs (hours),

subsequently media was replaced with 200µL of fresh medium containing eight various concentrations of AZM, Au-AZM and Ag-AZM (3.9-500µg/mL) placed in triplicates. Afterwards these treated cells were incubated in a humidified incubator with 5% CO_2 at the temperature of 37°C for 48 hours followed by aspiration of media and addition of 50µL of MTT dye (0.5mg/mL) per well for further incubation of 4 hours. Finally, DMSO (100µL) was transferred to wells in order to solubilize formazan crystals. The amount of dye reduction into formazan within cells was quantified by measuring absorbance at 570 nm by means of micro plate reader *(Spectra Max plus, Molecular devices, CA, USA)* as described (Luo *et al*., 2010). The cytotoxic effects of different treatment on HepG2 cells was expressed as (IC_{50}) i.e, the concentration causing 50% growth inhibition of cells.

Nuclear condensation

Analysis of HepG2 cells for nuclear fragmentation was performed after treating the cells with AZM, Au-AZM and Ag-AZM. For this experiment 30,000 cells per well were seeded in 24 well cell culture plate. After growth, cells were treated with test compounds and incubated for 48 hrs. Afterwards, cells were secured with 4% paraformaldehyde followed by washing with PBS and staining with DAPI *(4,6-diamidino-2-phenylindole) (MP Biomedical, Inc, USA)* which is a fluorescent binding dye. Treated cells were then observed under fluorescent microscope Nikon Ts2R-FL Inverted Research Microscope. Images taken were finally processed under ImageJ software (DeCoster, 2007) for determining Nuclear area factor i.e., circulatory 4 pi (area/perimeter^2) and roundness (perimeter2)/(4*pi*area).

STATISTICAL ANALYSIS

Data was analysed using SPSS program (version 20). Quantitative values in all of the groups were represented as mean ± S.E of mean (SEM) which were generated by ANOVA (Analysis of variance). Tukey's post hoc tests was then applied for inter group comparison. P-value < 0.05 was considered significant.

RESULTS

Synthesis and characterization of azithromycin coated gold and silver nanoparticles

AZM coated gold and silver nano-particles were synthesized by the reduction of ions in the presence of azithromycin as depicted in scheme 1b and 2b respectively. Upon addition of reducing agent $NaBH_4$, the colour of the reaction mixture converted from translucent to deep red indicative of synthesis of azithromycin coated gold nano-particles (Au-AZM) while the other mixture changed from transparent to yellow representing the formation of silver nano-particles. The reaction mixture showed the characteristic surface plasmon resonance (SPR) band at 526 nm by UV-Visible analysis for AU-AZM as depicted in fig. 1a while Ag-AZM synthesis was confirmed by characteristic SPR band at 396 nm as depicted in fig. 2a.

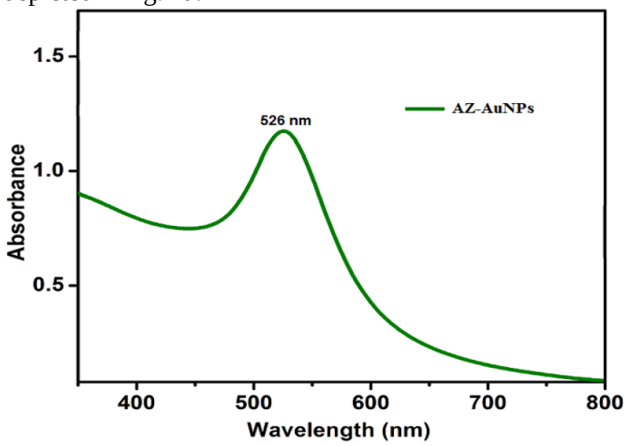

Fig. 1: UV-Visible spectrum of azithromycin coated gold nano-particles (AZ-AuNPs)

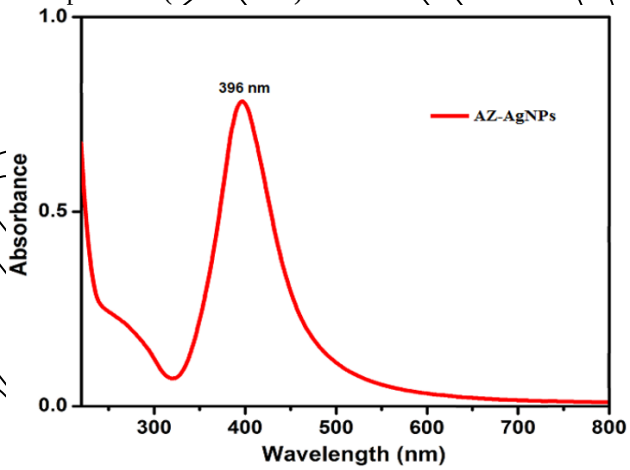

Fig. 2: UV-Visible spectrum of azithromycin coated silver nano-particles (AZ-AgNPs)

The expression of characteristic spectral bands, observed on FTIR spectroscopy confirms the nanomaterial–biomolecule conjugation, of AZM with gold and silver nanoparticles respectively. Fig. 3 shows the FTIR spectrum of azithromycin, AZM coated gold nanoparticles (Au-AZM) as pink trace while silver blue trace. The FTIR spectrum of AZM displayed characteristic peaks at 3324cm^{-1}, 2977cm^{-1}, 1723cm^{-1}, 1464cm^{-1}, 1377cm^{-1}, 1189cm^{-1} and 1048cm^{-1}. The peaks at 3324cm^{-1} and 2977cm^{-1} corresponds to the stretching vibrations of hydroxyl (O-H) and C-H groups. Stretching vibrational peaks at 1723cm^{-1}, 1464 cm^{-1} and 1377 cm^{-1} are attributed to the carbonyl (C=O) group and bending frequencies of CH_2 and CH_3 groups, respectively. The peaks at 1213cm^{-1} and 1048 cm^{-1} are appearing due to the stretching vibrations of C-N and C-O bonds. The FTIR spectrum of AZM coated gold nanoparticles (Au-AZM) showed significant peak at 3330cm^{-1} which represents the hydroxyl groups in nanoparticles.

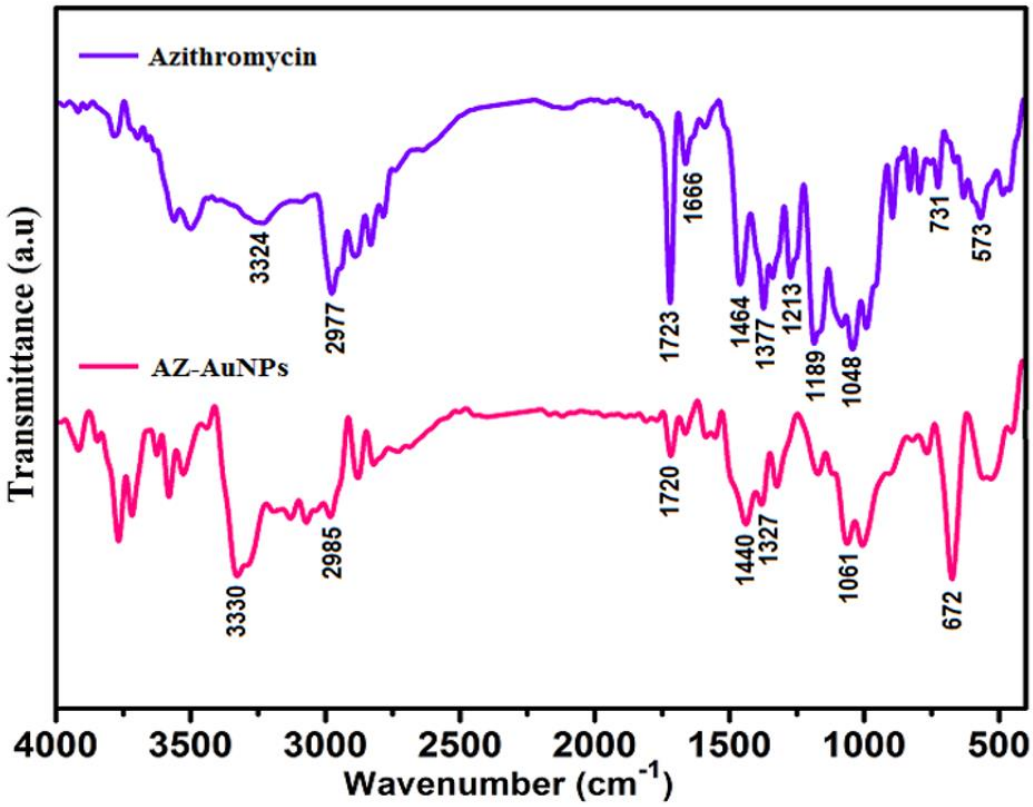

Fig. 3: FTIR spectrum of AZM (purple trace) and AZM coated gold nanoparticles (Au-AZM) (pink trace)

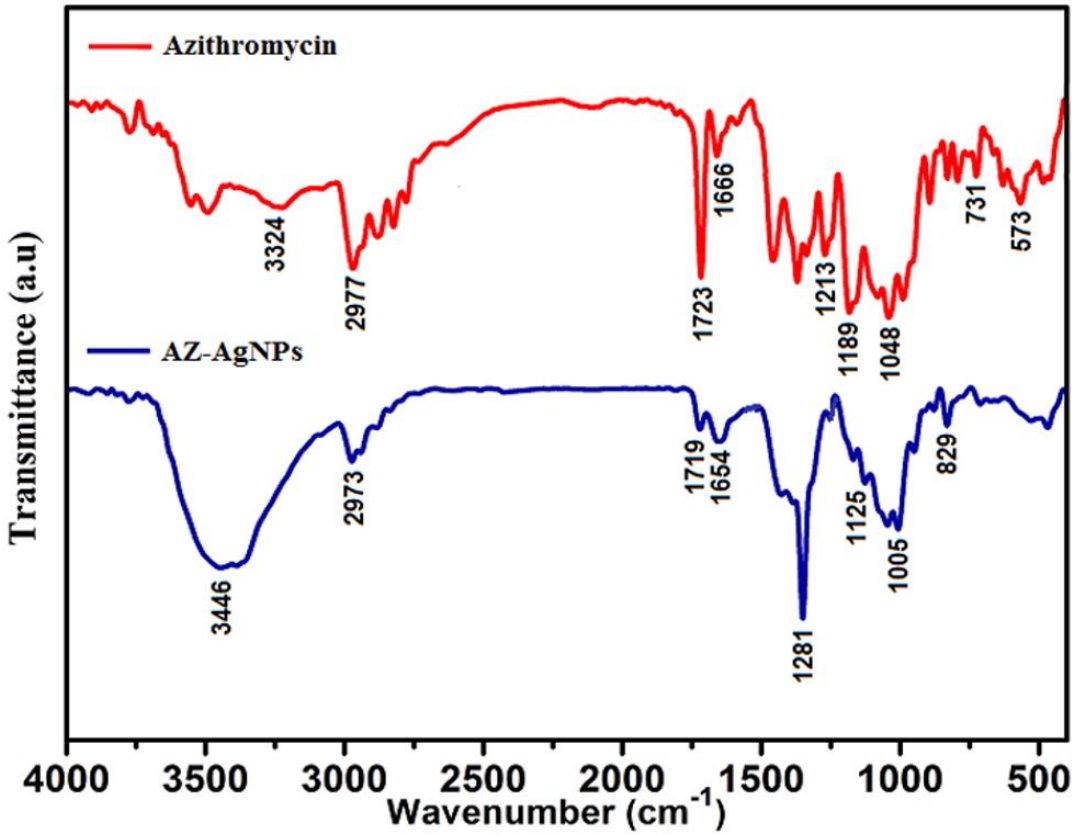

Fig. 4: FTIR spectrum of AZM (red trace) and AZM coated silver nanoparticles (Ag-AZM) (blue trace)

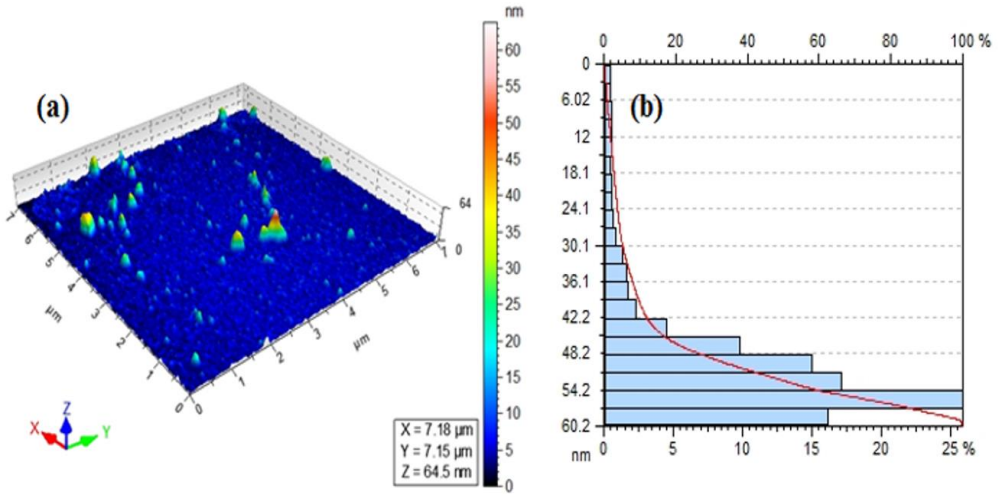

Fig. 5: AFM image of azithromycin coated gold nano-particles (Au-AZM) (a) 3-D height image and (b) average particle height distribution graph

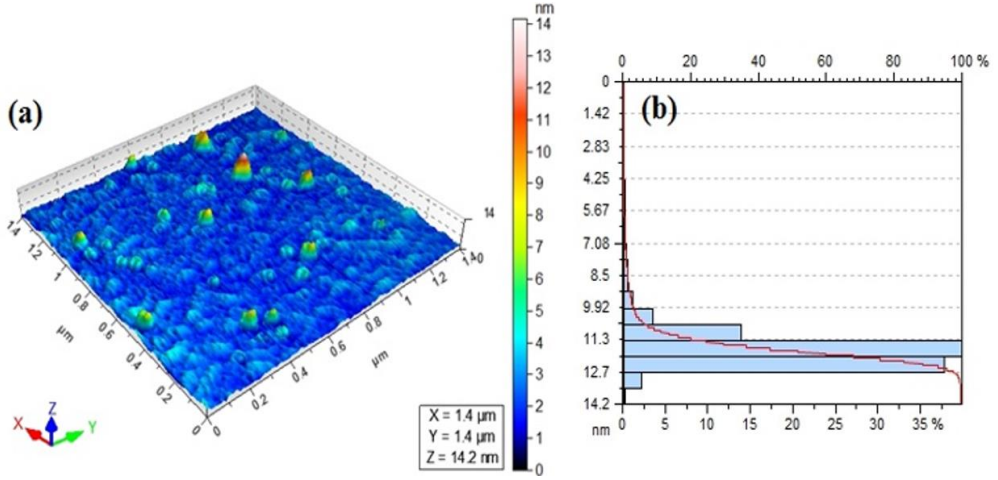

Fig. 6: AFM image of azithromycin coated silver nano-particles (Ag-AZM) (a) 3-D height image and (b) average particle height distribution graph.

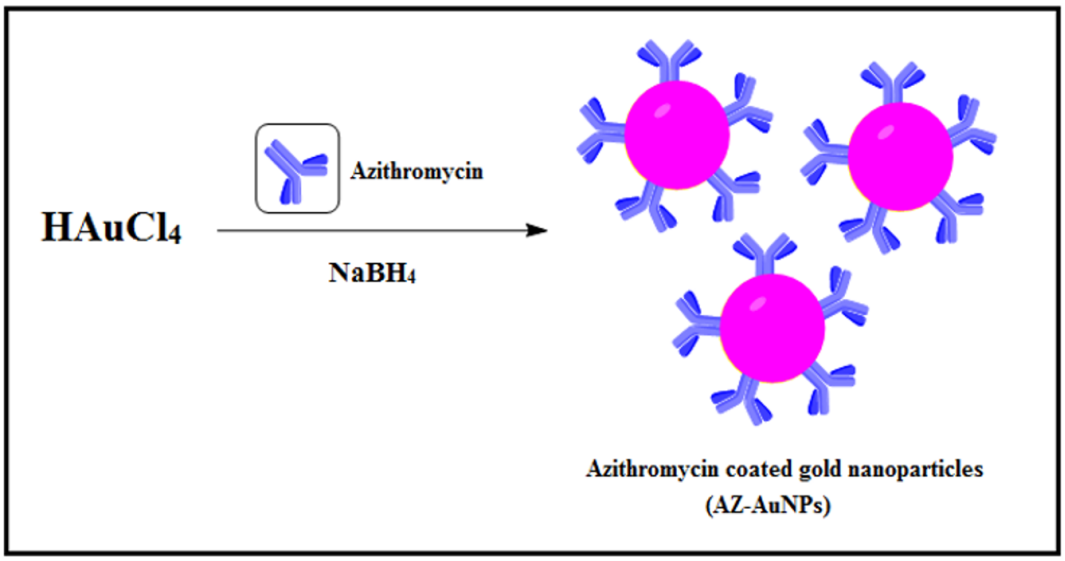

Scheme 1b: Synthesis of azithromycin coated gold nano-particles (Au-AZM)

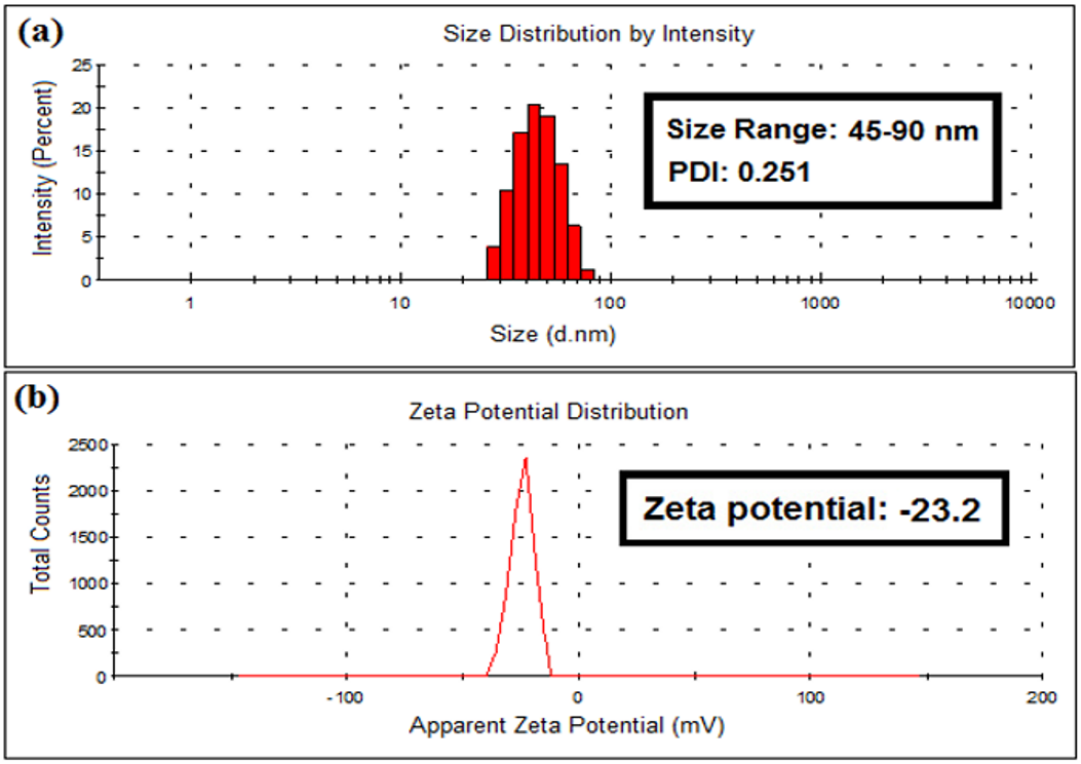

Fig. 7: Average particle size distribution histogram of AZM coated gold nano-particles (Au-AZM) (a) and zeta potential graph (b)

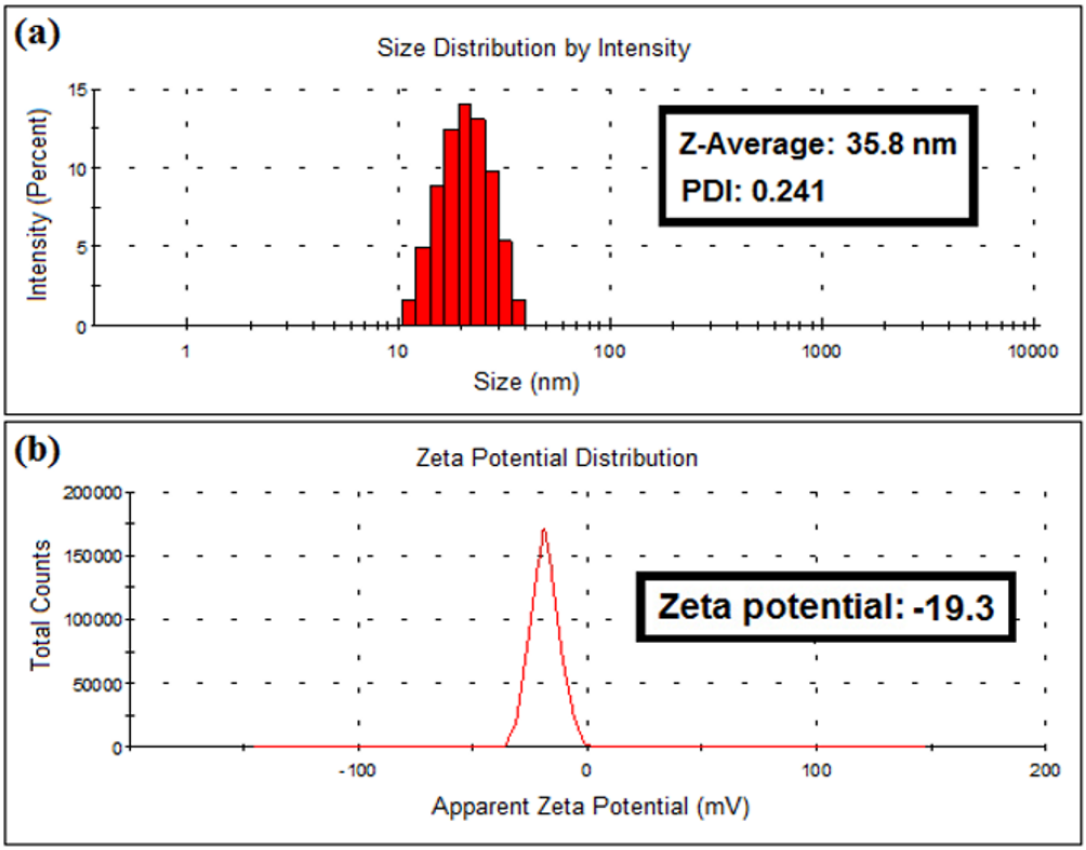

Fig. 8: Average particle size distribution histogram of AZM coated silver nano-particles (Ag-AZM) (a) and zeta potential graph (b)

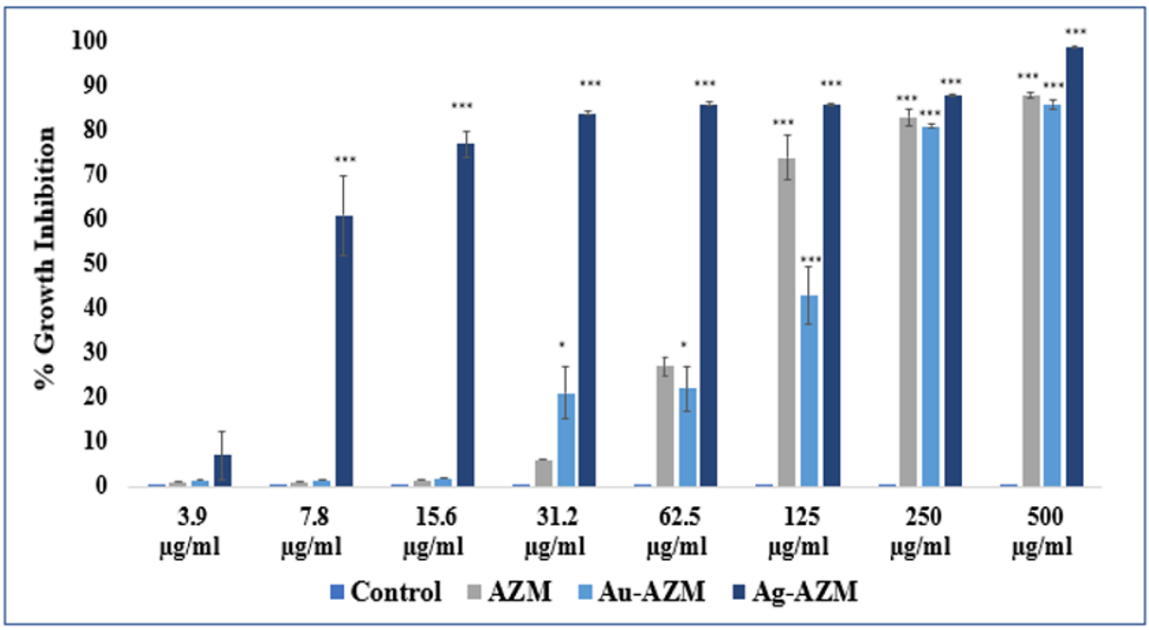

Fig. 9: Cytotoxic effects of AZM, Au-AZM and Ag-AZM on HepG2 cells after 48 hrs of treatment. The bar-graph depicts the concentration dependent inhibitory effects of AZM on growth of HepG2 cells. Significant difference in AZM and Au-AZM treated cells was observed and indicated as ***P<0.001 at 125, 250 and 500µg/ml while Ag-AZM showed significant ***P<0.001 inhibition at all concentrations except the lowest concentration 3.9 µg/mL as compared to un-treated group. *Each bar represents mean ± SEM for the experiments run in triplicates*

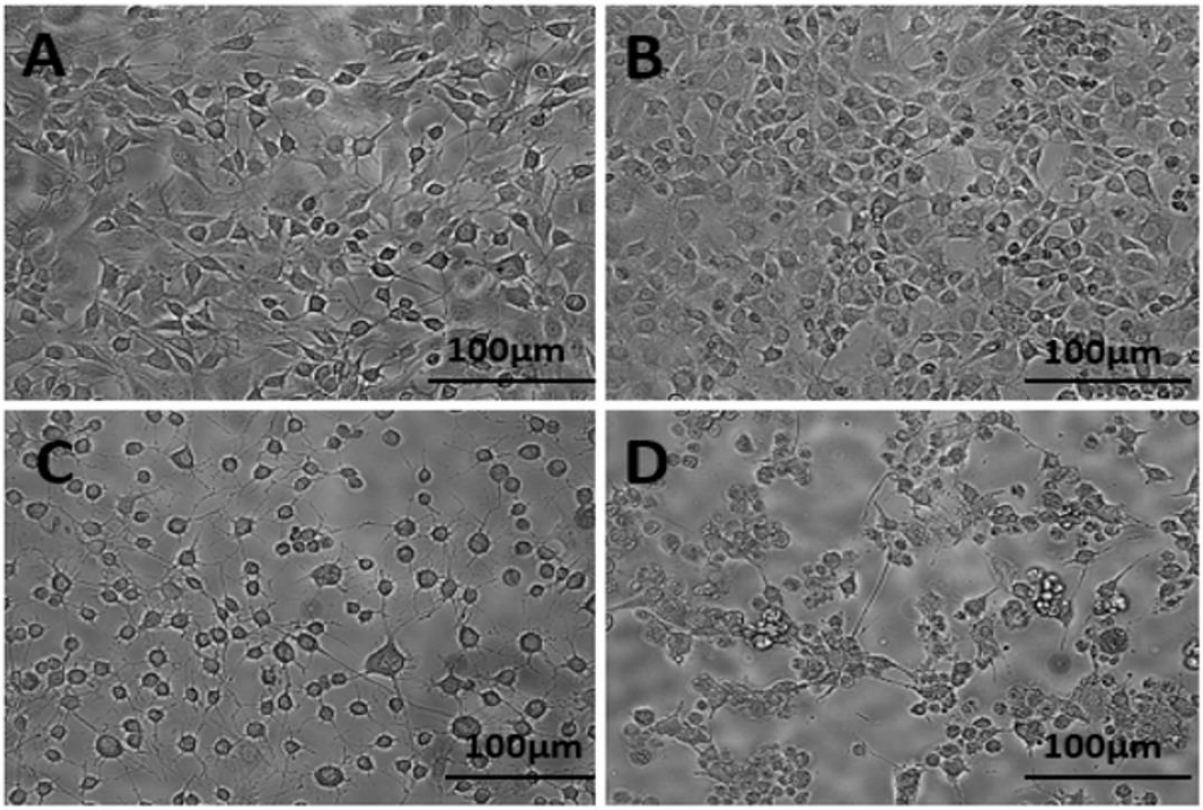

Fig. 10: *Inverted phase microscopy* displaying HepG2 cells, Control/un-treated (A), AZM (B), Au-AZM (C) and Ag-AZM (D) treated cells. The control cells (A) display regular morphology of cells. In contrast, cells treated with AZM (B), Au-AZM (C) and Ag-AZM (D) at IC_{50} concentrations show morphological changes as compared to control. *Images were taken at 10X magnification by using Floid cell imaging system, Thermo scientific, USA. Scale bar is 100µm.*

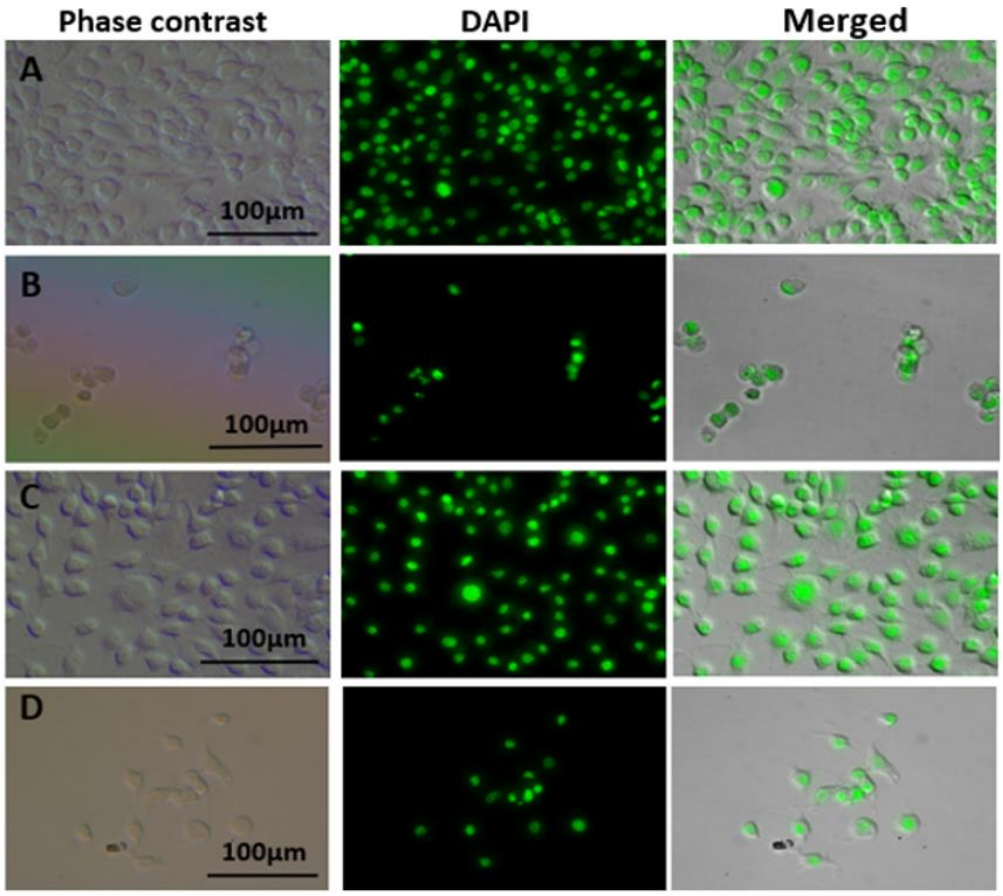

Fig. 11: Fluorescence microscopy showing DAPI stained nuclei of HepG2 cells and merged images by processing with Adobe Photoshop Version 7.0. Control (A), AZM (B) Au-AZM (C) and Ag-AZM (D) treated cells displaying significant results. *Fluorescence microscopy was done at 10X magnification using Nikon Ts2R-FL Inverted Research Microscope, Japan. Scale bar was 100µm.*

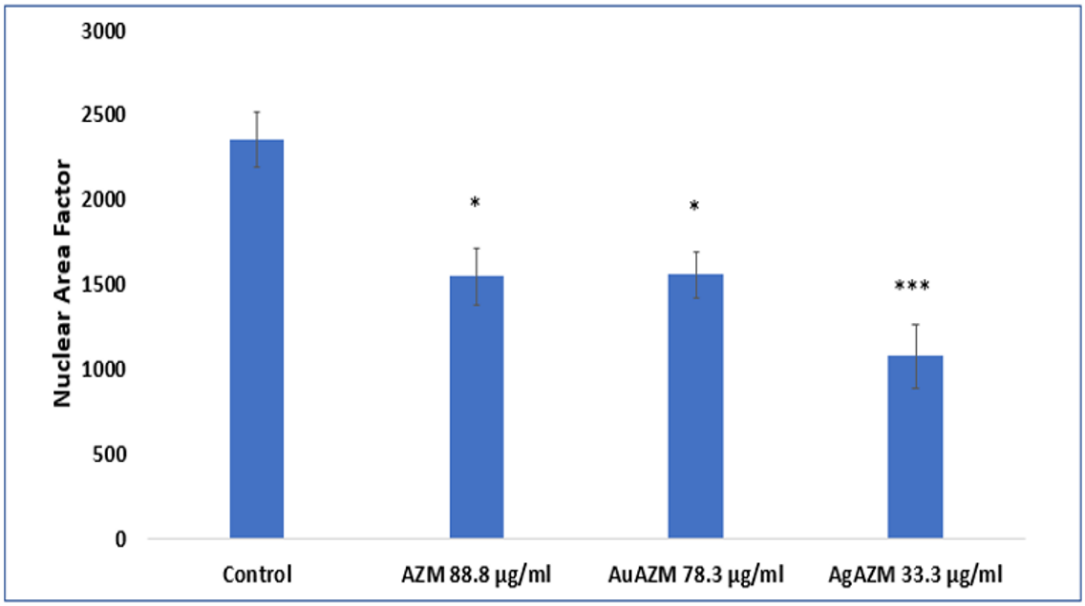

Fig. 12: Comparison of nuclear area factor after AZM, Au-AZM and Ag-AZM treatment induced apoptosis in DAPI stained HepG2 cells. ImageJ software was used for calculating circularity 4 pi (area/perimetre^2) and roundness (perimeter^2)/(4*pi*area). Nuclear area factor was calculated as the product of object area (in pixels2)*roundness. *Data was presented as mean ± SEM and experiments were run in triplicates.*

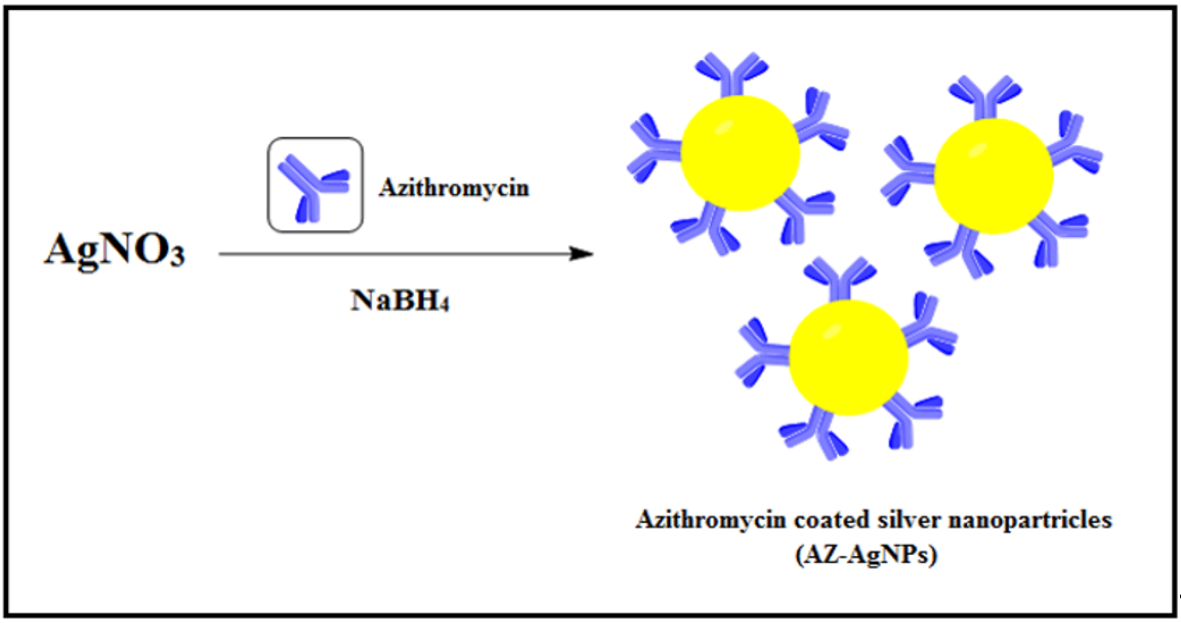

Scheme 2b: Synthesis of azithromycin coated silver nano-particles (Ag-AZM)

The reduction and shifting of peak of carbonyl group at 1720 cm^{-1} indicated the conjugation of carbonyl group of AZM with gold nanoparticles. The peaks at 1440 cm^{-1} and 1327 cm^{-1} were apparent due to the bending frequencies of CH_2 and CH_3 groups, respectively. Stretching frequency at 1061cm^{-1} is attributed to the stretching vibration of C-O bond. While AZM coated silver nanoparticles (Ag-AZM) showed a broad stretching vibrational peak at 3446 cm^{-1} which is appearing due to the greater hydrogen bonding by the presence of hydroxyl groups in the sample. The peak at 2973 cm^{-1} corresponds to the C-H groups of AZM. The sifting and reduction in the peak of carbonyl (C=O) group at 1719 cm^{-1} indicates the involvement and conjugation of this group with silver nanoparticles. The peaks at 1281 cm^{-1} and 1005 cm^{-1} are attributed to the shifting of C-N group and C-O group stretching vibrations. The FTIR spectrum results confirmed the successful conjugation of AZM with both gold and silver nanoparticles respectively.

Atomic force microscopic analysis was performed for the determination of morphological analysis of azithromycin coated gold and silver nanoparticle. The results are given in fig. 5 & 6. fig. 5a shows that the nanoparticles have pointed shape and were well dispersed having an average height in the range of 48-60 nm while on the other hand fig. 6a depicted that the nanoparticles have spherical shape and were uniformly distributed. The particles height distribution of AZ-AgNPs was in the range of 9-13 nm.

The zeta sizer and potential analysis was carried out for the determination of particle size distribution of both AZM coated gold and silver nanoparticles. fig. 7(a) shows that the Au-AZM have particle size within range of 45-90 nm poly dispersity index of 0.251 while average particles size distribution of Ag-AZM was found in the range of 35.8 nm having poly dispersity index (PDI) of 0.241 (fig. 8a). The poly dispersity index indicate that the nanoparticles have uniform size distribution. The zeta potential analysis of Au-AZM was found to be -23.2 (fig. 7b) while for Ag-AZM it was found to be -19.3mV (fig. 8b). This negative zeta potential value indicate the stability of these nanoparticles due to greater repulsion between nanoparticles.

Cytotoxic Effect of AZM, Au-AZM and Ag-AZM on HepG2 Cells

Effects of AZM, Au-AZM and Ag-AZM were evaluated against hepatocellular cancer (HepG2) cell line utilizing MTT assay for all treatment groups at different concentrations. AZM, Au-AZM and Ag-AZM inhibited the proliferating HepG2 cells with an IC_{50} value of 88.8, 78.3 and 33.3 µg/mL respectively. The Ag-AZM was the most potent inhibitor among all (fig. 9)

Morphology of AZM, Au-AZM and Ag-AZM treated cells

The effect of AZM, Au-AZM and Ag-AZM on morphological appearance of HepG2 cells was analyzed using inverted phase microscope following 48 hours of treatment with AZM, Au-AZM and Ag-AZM at their IC_{50} concentrations. The Au-AZM and Ag-AZM cells showed noteworthy morphological aberrations as compare to un-treated group (fig. 10).

Effect of AZM, Au-AZM and Ag-AZM on nuclear condensation of HepG2

The effects of AZM, Au-AZM and Ag-AZM on nuclear changes were analyzed by DAPI staining. Fragmentation of nuclei and shrinkage in nuclear area factor are morphological hall marks of apoptosis. After 48 hrs of treatment with AZM, Au-AZM and Ag-AZM at IC_{50}

concentrations, cells were observed for nuclear changes (fig. 11) and reduction in nuclear area factor (fig. 12) came out significant for AZM and Au-AZM with P-value of <0.05 while highly significant for Ag-AZM with P-value of <0.001.

DISCUSSION

In the present study, AZM was preferentially selected for nano conjugation over other macrolides owing to its differential properties of minimal capacity to inhibit CYP450 enzyme system, having long half-life and superior anti-inflammatory, anti-proliferatory, immunomodulatory and autophagic activities more than its congeners (Mukai *et al*, 2016). Azithromycin, one of the safest macrolide has been studied in combination with recommended anticancer drugs for their anticipated synergistic activity previously in colon (Qiao *et al*, 2018), cervical and gastric cancer (Zhou *et al*, 2012). Moriya *et al* also reported anticancer effect of Azithromycin on multiple myeloma cell lines (U266, IM-9 and RPMI8226) both alone and in combination with Bortezomib which showed enhanced the BZ-induced cytotoxicity when combined with AZM (Moriya *et al*, 2013).

The utilization of nano-particles in biomedical industry is diverse i.e. in diagnostics, therapeutics, theragnostic etc. Owing to their distinct features such as greater surface area, substantial physical properties and enhance permeability and retention effect (EPR), the metallic nanoparticles such as gold and silver are considered very important and interesting candidates for several clinical diagnostic and therapeutic applications (Nene and Nyokong, 2023).

AZM conjugated gold and silver nano-particles were synthesized by the aqueous solution reduction method using NaBH4 as a reductant due to its robust reducing capability (Padole *et al*, 2024).

To the best of our literature search, very first time we conjugated silver and gold nanoparticles with AZM and tested against HepG2 cell line, and our results corroborated the rationalized use of nano particles in certain cancers (Deng *et al*, 2023). Gold nano shells have been utilized as theragnostic in breast cancer *in vitro* (Bardhan *et al*, 2010) while another study has directed the multi-functional proficiencies of gold nano-conjugates of anticancer agent Doxorubicin for therapy of prostatic cancer, where enhanced targeted killing of cancer cells were reported (Kim *et al*, 2010).

When MTT assay was performed for cytotoxic analysis of gold (Au) and silver (Ag) conjugated AZM at different concentrations, the IC_{50} obtained for Ag-AZM came out to be 33.3µg/mL which was more effective as compared to Au-AZM having IC_{50} of 78.8µg/mL nearly equal to AZM alone (IC50=88.3µg/mL) (fig. 9).

Studies are rather scarce regarding assessment of anticancer effects of conventional drugs/ antimicrobials with nano conjugates particularly related to metallic nano particles, nevertheless certain studies support our findings.

According to a study conducted by Karuppiah *et al*, silver conjugated Doxorubicin tested against MDA-MB-453(TNBC breast cancer) cell line resulted in excellent cell inhibition rate compared to conventional form of Doxorubicin owing to reduced size and spherical morphology of nanoparticles (Karuppaiah *et al*, 2020).

Moreover, silver nanoparticles when combined with Wortmannin induced cytotoxicity in B16 mouse melanoma cells via increased ROS production which led eventually to apoptotic death of cells (Lin *et al*, 2014).

In previuos study, trastuzumab when conjugated with gold compounds maintained their affinity towards HER2 breast cancer cell line. These gold conjugated trastuzumab was found to be more cytotoxic to cancer cells than trastuzumab and gold complexes alone (Curado *et al*, 2019).

DAPI staining used for evaluation of apoptotic potential of compounds which showed significant inhibition with Au-AZM (P-value<0.05) while Ag-AZM show highly significant apoptosis with p-value of (<0.001) at their respective IC_{50} concentration (fig. 12).

Further the effects of peptide-nanoconjugates of AuNp and AgNp were tested on colon cancer HT-29 and breast cancer MDA MB-231 cell lines, where both the conjugations demonstrated chromatin condensation and nuclear clumping of cancer cells (Banerjee *et al*, 2019).

From above standpoints it is apparent that cancer cell type being treated, physiochemical properties of nanoparticle and pharmacodynamics of drugs themselves are prime factors on which the anticancer efficacy of nanoparticles are reliant. Therefore, extensive mechanistic studies will be defensible to second our findings before leading to *in-vivo* studies.

CONCLUSION

The present investigation showed the synthesis as well as characterization of AZM conjugated gold and silver nanoparticles. This *in vitro* study also discovered augmented anticancer effects of Ag-AZM as evident by decreased IC_{50} and revealed apoptotic activity in HepG2 cell line when compared to Au-AZM, however preclinical and clinical trials are obligatory in order to label it as an effective therapeutic agent against HCC.

LIMITATION

The findings of our study need to be corroborated through *in vivo* experiments using animal models. Furthermore,

underlying molecular mechanisms responsible for apoptotic activity of tested compounds against cancer cell line also required to be investigated.

REFERENCES

Abbaszadeh S, Nikbakht M, Ramezannezhad P, Farahani MS, Ahmadi SAY and Safarzadeh A (2019). Some issues of nanometals applications in cancer treatment. *International Journal of Biology and Chemistry*, **12**(2): 49-55.

Alrushaid N, Khan FA, Al-Suhaimi EA and Elaissari A (2023). Nanotechnology in cancer diagnosis and treatment. *Pharmaceutics*, **15**(3): 1025.

Banerjee K, Ravishankar Rai V and Umashankar M (2019). Effect of peptide-conjugated nanoparticles on cell lines. *Progress in biomaterials*, **8**: 11-21.

Baranwal J, Barse B, Di Petrillo A, Gatto G, Pilia L and Kumar A (2023). Nanoparticles in cancer diagnosis and treatment. *Materials*, **16**(15): 5354.

Bardhan R, Chen W, Bartels M, Perez-Torres C, Botero MF, McAninch RW, Contreras A, Schiff R, Pautler RG, Halas NJ and Joshi A (2010). Tracking of multimodal therapeutic nanocomplexes targeting breast cancer *in vivo*. *Nano letters*, **10**(12): 4920-4928.

Chatterjee P and Kumar S (2022). Current developments in nanotechnology for cancer treatment. *Materials Today: Proceedings*, **48**: 1754-1758.

Curado N, Dewaele-Le Roi G, Poty S, Lewis JS and Contel M (2019). Trastuzumab gold-conjugates: Synthetic approach and *in vitro* evaluation of anticancer activities in breast cancer cell lines. *Chemical Communications*, **55**(10): 1394-1397.

DeCoster MA (2007). The nuclear area factor (NAF): A measure for cell apoptosis using microscopy and image analysis. *Modern research and educational topics in microscopy*, **1**: 378-384.

Deng G, Zha H, Luo H and Zhou Y (2023). Aptamer-conjugated gold nanoparticles and their diagnostic and therapeutic roles in cancer. *Frontiers in Bioengineering and Biotechnology*, **11**: 1118546.

Karuppaiah A, Rajan R, Ramanathan M and Nagarajan A (2020). Cytotoxicity and synergistic effect of biogenically synthesized ternary therapeutic nano conjugates comprising plant active principle, silver and anticancer drug on MDA-MB-453 breast cancer cell line. *Asian Pacific Journal of Cancer Prevention: APJCP*, **21**(1): 195.

Khursheed R, Dua K, Vishwas S, Gulati M, Jha NK, Aldhafeeri GM, Alanazi FG, Goh BH, Gupta G, Paudel, KR and Hansbro PM (2022). Biomedical applications of metallic nanoparticles in cancer: Current status and future perspectives. *Biomedicine & pharmacotherapy*, **150**: 112951.

Kim D, Jeong YY and Jon S (2010). A drug-loaded aptamer-gold nanoparticle bioconjugate for combined CT imaging and therapy of prostate cancer. *ACS nano*, **4**(7): 3689-3696.

Lin J, Huang Z, Wu H, Zhou W, Jin P, Wei P, Zhang Y, Zheng F, Zhang J, Xu J and Hu Y (2014). Inhibition of autophagy enhances the anticancer activity of silver nanoparticles. *Autophagy*, **10**(11): 2006-2020.

Liu J, Guo L, Mi Z, Liu Z, Rong P and Zhou W (2022). Vascular bursts-mediated tumor accumulation and deep penetration of spherical nucleic acids for synergistic radio-immunotherapy. *Journal of Controlled Release*, **348**: 1050-1065.

Luo J, Li YN, Wang F, Zhang WM and Geng X (2010). S-adenosylmethionine inhibits the growth of cancer cells by reversing the hypomethylation status of c-myc and H-ras in human gastric cancer and colon cancer. *International journal of biological sciences*, **6**(7): 784.

Male KB, Li J, Bun CC, Ng SC and Luong JH (2008). Synthesis and stability of fluorescent gold nanoparticles by sodium borohydride in the presence of mono-6-deoxy-6-pyridinium-β-cyclodextrin chloride. *The Journal of Physical Chemistry C*, **112**(2): 443-451.

Moriya S, Che XF, Komatsu S, Abe A, Kawaguchi T, Gotoh A, Inazu M, Tomoda A and Miyazawa K (2013). Macrolide antibiotics block autophagy flux and sensitize to bortezomib via endoplasmic reticulum stress-mediated CHOP induction in myeloma cells. *International journal of oncology*, **42**(5): 1541-1550.

Mukai S, Moriya S, Hiramoto M, Kazama H, Kokuba H, Che XF, Yokoyama T, Sakamoto S, Sugawara A, Sunazuka T and Ōmura S (2015). Macrolides sensitize EGFR-TKI-induced non-apoptotic cell death via blocking autophagy flux in pancreatic cancer cell lines. *International journal of oncology*, **48**(1): 45-54.

Nene LC and Nyokong T (2023). Enhancement of the in vitro anticancer photo-sonodynamic combination therapy activity of cationic thiazole-phthalocyanines using gold and silver nanoparticles. *Journal of Photochemistry and Photobiology A: chemistry*, **435**: 114339.

Padole NN, Majgavali NV, Meshram MA and Padole NN (2024). Spectroscopic Study of Synthesized Copper Nanoparticles by Chemical Reduction Method. *Asian Journal of Pharmaceutical Research and Development*, **12**(1): 10-14.

Pang Y, Eresen A, Zhang Z, Hou Q, Wang Y, Yaghmai V and Zhang Z (2022). Adverse events of sorafenib in hepatocellular carcinoma treatment. *American Journal of Cancer Research*, **12**(6): 2770.

Qiao X, Wang X, Shang Y, Li Y and Chen SZ (2018). Azithromycin enhances anticancer activity of TRAIL by inhibiting autophagy and up-regulating the protein levels of DR4/5 in colon cancer cells in vitro and in vivo. *Cancer Communications*, **38**: 1-13.

Shariatzadeh S, Moghimi N, Khalafi F, Shafiee S, Mehrabi M, Ilkhani S, Tosan F, Nakhaei P, Alizadeh A,

Varma RS and Taheri M (2022). Metallic nanoparticles for the modulation of tumor microenvironment; a new horizon. *Frontiers in Bioengineering and Biotechnology*, **10**: 847433.

Tahir, M., 2022. Hepatocellular carcinoma: Hope and challenges. *CA Cancer J Clin*, **72**(7): pp.----?

Tian H, Zhang T, Qin S, Huang Z, Zhou L, Shi J, Nice EC, Xie N, Huang C and Shen Z (2022). Enhancing the therapeutic efficacy of nanoparticles for cancer treatment using versatile targeted strategies. *Journal of hematology & oncology*, **15**(1): 132.

Xu JJ, Zhang WC, Guo YW, Chen XY and Zhang YN, (2022). Metal nanoparticles as a promising technology in targeted cancer treatment. *Drug Delivery*, **29**(1): 664-678.

Zhang Z, Shen W, Xue J, Liu Y, Liu Y, Yan P, Liu J and Tang J (2018). Recent advances in synthetic methods and applications of silver nanostructures. *Nanoscale Research Letters*, **13**: pp.1-18.

Zhou X, Zhang Y, Li Y, Hao X, Liu X and Wang Y (2012). Azithromycin synergistically enhances anti-proliferative activity of vincristine in cervical and gastric cancer cells. *Cancers*, **4**(4): 1318-1332.